Journal of the European Ceramic Society 36 (2016) 625–629

Contents lists available at www.sciencedirect.com

Journal of the European Ceramic Society

journal homepage: www.elsevier.com/locate/jeurceramsoc

Novel series of ultra-low loss microwave dielectric ceramics: $Li_2Mg_3BO_6$ (B = Ti, Sn, Zr)

Zhifen Fu[a,b,*], Peng Liu[a,*], Jianli Ma[b], Xiaogang Zhao[a], Huaiwu Zhang[c]

[a] College of Physics and Information Technology, Shaanxi Normal University, Xi'an 710062, China
[b] College of Science, Anhui University of Science and Technology, Huainan 232001, China
[c] The Key Laboratory of Electronic Thin Film and Integrated devices, University of Electronic Science and Technology of China, Chengdu 610054, China

ARTICLE INFO

Article history:
Received 25 May 2015
Received in revised form 14 October 2015
Accepted 26 October 2015
Available online 11 November 2015

Keywords:
Microwave dielectric properties
Microstructure
$Li_2Mg_3BO_6$ (B = Ti, Sn, Zr) Ceramics

ABSTRACT

Using a conventional solid-state reaction $Li_2Mg_3BO_6$ (B = Ti, Sn, Zr) ceramics were prepared and their microwave dielectric properties were investigated. The analysis revealed that cubic $Li_2Mg_3BO_6$ (B = Ti, Sn, Zr) ceramics with a rock salt structure could be obtained in their respective sintering temperature range. Three promising ceramics $Li_2Mg_3TiO_6$, $Li_2Mg_3SnO_6$ and $Li_2Mg_3ZrO_6$ sintered at 1280 °C, 1360 °C and 1380 °C possessed out-bound microwave dielectric properties: ϵ_r = 15.2, 8.8 and 12.6, $Q \times f$ = 152,000 GHz (at 8.3 GHz), 123,000 GHz (at 10.7 GHz) and 86,000 GHz (at 9.3 GHz), and τ_f = −39 ppm/°C, −32 ppm/°C and −36 ppm/°C, respectively.

1. Introduction

Microwave dielectric ceramics are indispensable components in wireless communication due to their characteristics of compactness, light weight, thermal stability, low cost and excellent performance [1,2]. A variety of microwave devices have been developed using dielectric resonators as the frequency-determining components. Four characteristic properties are required from the device design point of view: (1) high quality factor (low dielectric loss, $Q \times f$ > 10,000 GHz) for selectivity, (2) low dielectric constant (ϵ_r < 15) to avoid signal delay, (3) small temperature coefficient of resonant frequency for stability, (4) low sintering temperature (T < 960 °C) to use cheaper and highly conductive internal electrode metals [3–6]. The search for the new materials, which satisfy all the above-mentioned requirements, is one of the major challenges faced by the electronic industry.

Recently, many dielectric material systems composed of TeO_2, Bi_2O_3, MoO_3, P_2O_5, Li_2O and V_2O_5 have been developed [7–12]. Among them, Li-containing compounds such as Li_2WO_4, Li_2CeO_3, Li3AO4 (A = Nb, Ta, Sb), and Li_2TiO_3 have gained considerable attention due to their excellent microwave dielectric properties [13–16]. Li_2TiO_3 ceramics, which have promising microwave dielectric properties of ϵ_r = 20-24, $Q \times f$ = 40,000–70,000 GHz, and τ_f = +(20–30) ppm/°C, exhibit rock salt structure [17,18]. By the substitution of Ti lattice atoms in Li_2TiO_3 with Sn, Zr and Mn, $Li_2Sn(Zr, Mn)O_3$ ceramics with similar rock salt structure were obtained and demonstrated superior dielectric properties [19,20].

$Li_2Mg_3SnO_6$ with a face-centred-cubic rock salt structure was reported by Keulen et al. [21,22]. However, microwave dielectric properties of $Li_2Mg_3SnO_6$ ceramic have not been investigated as yet. Because of the similar Shannon's effective ionic radii and identical charge of Ti^{4+} [Radius = 0.605 Å, Coordination number (CN) = 6], Zr^{4+} (radius = 0.72 Å, CN = 6) and Sn^{4+} (radius = 0.69 Å, CN = 6), it is worthwhile to synthesize $Li_2Mg_3BO_6$ (B = Ti, Sn, Zr) ceramic. In this study, the crystal phase, microstructure, and microwave dielectric properties of $Li_2Mg_3BO_6$ (B = Ti, Sn, Zr) ceramics were investigated.

2. Experimental procedure

$Li_2Mg_3BO_6$ (B = Ti, Sn, Zr) ceramics samples were prepared by the conventional solid-state method. Li_2CO_3 (98%), MgO (99.99%), TiO_2 (99.99%), SnO_2 (99.5%) and ZrO_2 (99.99%) powders were used as precursors. Stoichiometric amounts of the powder samples were mixed and ball milled using ZrO_2 balls in ethanol for 10 h. All mixtures were dried and calcined at 1000–1200 °C for 4 h. Subsequently, the calcined powders were reground for 8 h, dried, mixed with 5 wt% PVA as a binder and granulated. Afterwards, the powders were uniaxially pressed into pellets with 11.5 mm in diameter and 5–6 mm in height under the pressure of 200 MPa. These pellets

* Corresponding author at: College of Physics and Information Technology, Shaanxi Normal University, Xi'an 710062, China. Fax: +86 29 85303823.
E-mail addresses: fuzhifen80@sina.com (Z. Fu), liupeng@snnu.edu.cn (P. Liu).

http://dx.doi.org/10.1016/j.jeurceramsoc.2015.10.040
0955-2219/

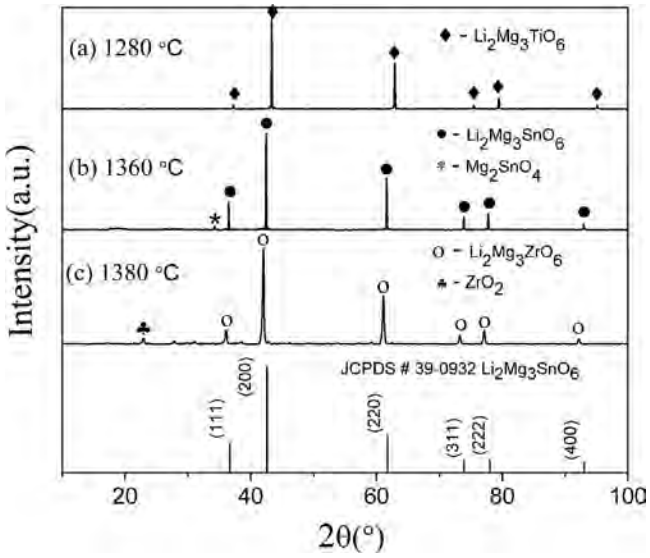

Fig. 1. XRD patterns of $Li_2Mg_3BO_6$ (B = Ti, Sn, Zr) ceramics sintered at optimum temperatures.

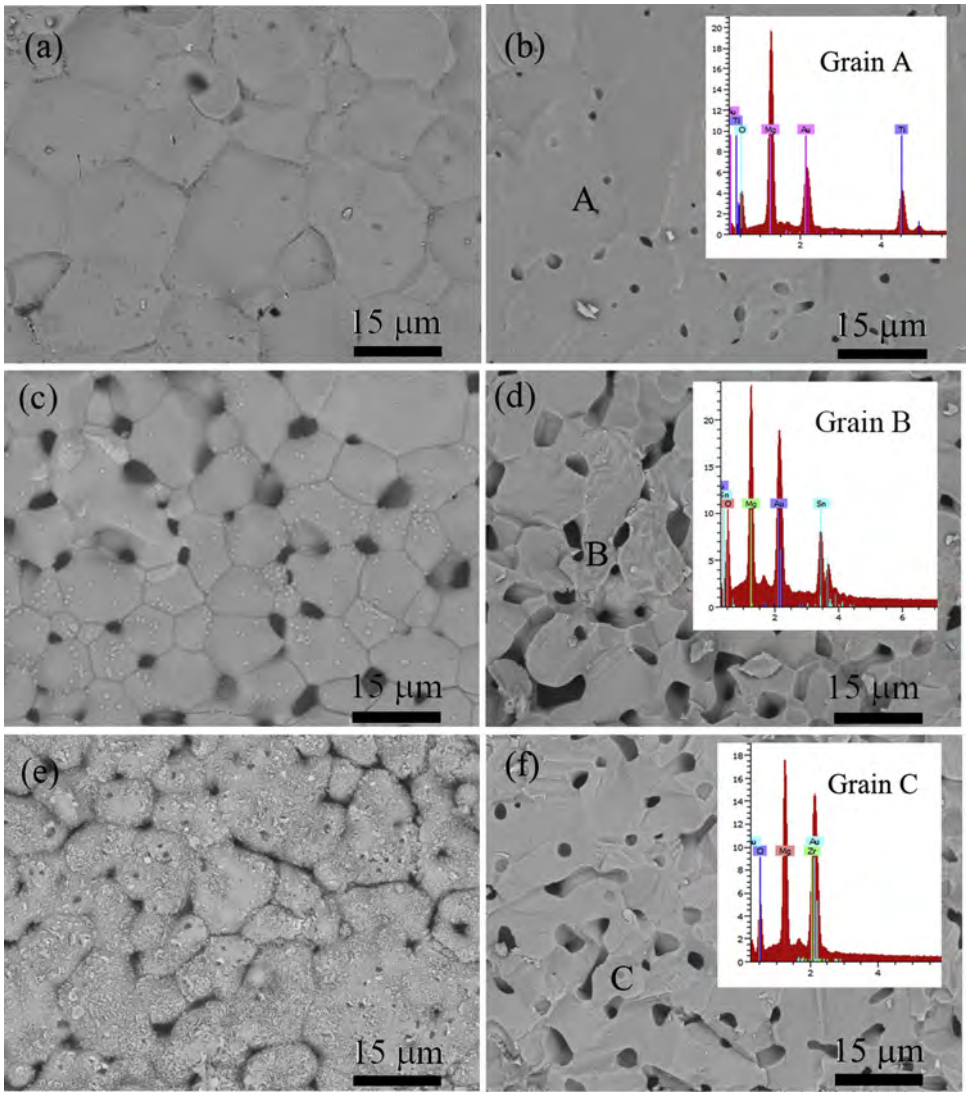

Fig. 2. SEM images of (a) as-fired and (b) fractured surface of $Li_2Mg_3TiO_6$ ceramics sintered at 1280 °C; (c) as-fired and (d) fractured surface of $Li_2Mg_3SnO_6$ ceramics sintered at 1360 °C; and (e) as-fired and (f) fractured surface of $Li_2Mg_3ZrO_6$ ceramics sintered at 1380 °C. Insets show the results of EDS of grain A, B, and C marked in (b), (d), (f), respectively.

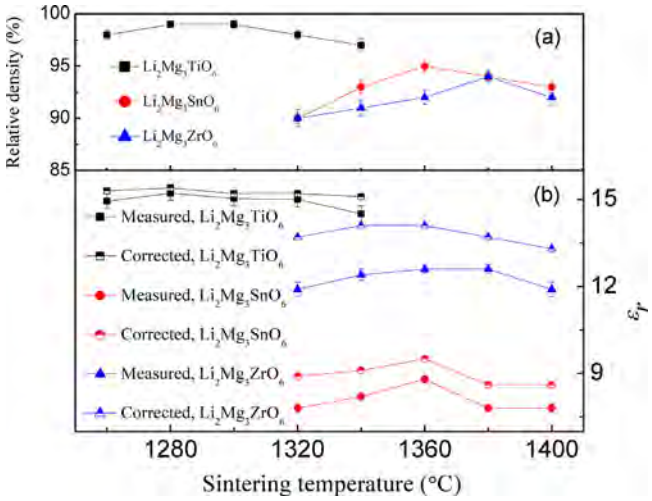

Fig. 3. (a) Relative density (b) ϵ_r of $Li_2Mg_3BO_6$ (B = Ti, Sn, Zr) ceramics as a function of sintering temperatures (including ± 2% error bars).

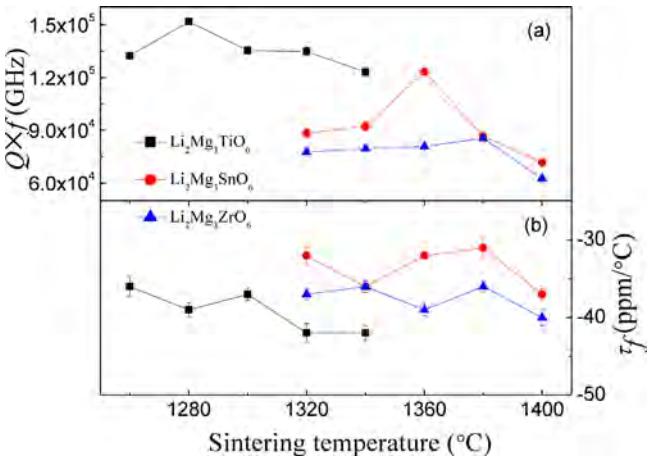

Fig. 4. Variations in (a) $Q \times f$, and (b) τ_f values of $Li_2Mg_3BO_6$ (B = Ti, Sn, Zr) ceramics at different sintering temperatures (including ± 4% error bars).

were sintered at 1260–1400 °C for 6 h with a temperature-ramping rate of 4 °C/min.

The bulk densities of the sintered ceramics were measured by Archimedes method. The crystal structures were analyzed using X-ray diffraction (XRD) with CuKα radiation (Rigaku D/MAX2550, Tokyo, Japan). The lattice parameters of specimens were calculated from XRD patterns by using the Jade 6.5 software. The microstructures were investigated using a scanning electron microscope (SEM, Quanta 200, FEI Company, Eindoven, Holland) coupled with energy dispersive X-ray spectroscopy (EDS). The microwave dielectric properties of the specimens were measured using a network analyzer (ZVB20, Rohde & Schwarz, Munich, Germany) with the $TE_{01\delta}$ shielded cavity method. The temperature coefficient resonant frequency (τ_f) was calculated with the following formula:

$$\tau_f = \frac{(f_2 - f_1) \times 10^6}{f_1 (T_2 - T_1)} \quad (1)$$

3. Results and discussions

Fig. 1 shows the XRD patterns of three types of $Li_2Mg_3BO_6$ (B = Ti, Sn, Zr) ceramics sintered at their optimized temperature of 1280 °C, 1360 °C and 1380 °C for 4 h, respectively. The XRD patterns were indexed according to *Fm-3m* (225) space group (JCPDS #39-0932). All samples exhibited the $Li_2Mg_3SnO_6$ cubic phase with ordered rock salt structure. All the peaks were well matched with the data of $Li_2Mg_3TiO_6$, $Li_2Mg_3SnO_6$ and $Li_2Mg_3ZrO_6$ phase. In addition, a little of impure phase of Mg_2SnO_4 and ZrO_2 was observed in Fig. 1(b) and (c), respectively. The lattice parameters of $Li_2Mg_3BO_6$ (B = Ti, Sn, Zr) ceramics calculated from XRD patterns were $a = b = c = 4.173(5)$ Å and $\beta = 90°$, $a = b = c = 4.254(5)$ Å and $\beta = 90°$, and $a = b = c = 4.293(6)$ Å and $\beta = 90°$, respectively. Compared with the XRD of the $Li_2Mg_3SnO_6$ phase, it was observed that the position of Fig. 1(a) peaks shifted slightly toward the higher angle due to the smaller ionic radius of Ti^{4+} ($R = 0.605$ Å) than that of Sn^{4+} ($R = 0.69$ Å), which lead to smaller lattice parameters of $Li_2Mg_3TiO_6$ than those of $Li_2Mg_3SnO_6$. In the same principle, the position of peaks in Fig. 1(c) shifted slightly towards the lower angle.

The surface morphology of as-fired and fractured $Li_2Mg_3BO_6$ (B = Ti, Sn, Zr) ceramics sintered at their optimized temperature are compared in Fig. 2. It can be seen that these three ceramics exhibited a porous structure. It is reported that lithium is volatile and evaporates at elevated sintering temperatures (≥1000 °C) [23]. The formation of pores in the matrix could be due to the evaporation of lithium, which was observed in the synthesis of Li2ATi3O8 (A = Mg, Zn) system as well [11]. The grain size of pure $Li_2Mg_3TiO_6$ ceramics sintered at 1280 °C lied in the range of 15–30 μm, and dense and fine microstructure was observed as shown in Fig. 2(a). The grain size of $Li_2Mg_3SnO_6$ ceramics sintered at 1360 °C was about 7–15 μm, and its microstructure did not look very dense and was more porous due to higher sintering temperature. Similar results are obtained for $Li_2Mg_3ZrO_6$ ceramics sintered at 1380 °C. Insets show the results of EDS of grains A, B, and C marked in Fig. 2(b), (d), (f), respectively. Based on the EDS analyses, the grains marked A, B and C were considered to be $Li_2Mg_3TiO_6$, $Li_2Mg_3SnO_6$, and $Li_2Mg_3ZrO_6$, respectively. The impurity phase detected by XRD was not visible in SEM.

Fig. 3 presents the relative density and dielectric constant (ϵ_r) of $Li_2Mg_3BO_6$ (B = Ti, Sn, Zr) ceramics sintered at various temperatures. The error was derived from the mean standard deviation and the error bars are plotted in Fig. 3. With increasing sintering temperature, the relative density of all specimens increased and reached a maximum value of 99% at 1280 °C, 95% at 1360 °C and 94% at 1380 °C, respectively. And then the relative density decreased as temperature increased further due to trapped porosity caused by the abnormal grain growth as well as evaporation of lithium at higher sintering temperature [23]. The dielectric constant (ϵ_r) is dependent on the density, dielectric polarizabilities, and structural characteristics such as phase composition, compositional homogeneity, and grain boundaries [24]. As potted in Fig. 3(b), the variation in measured dielectric constant values (ϵ_{meas}) with sintering temperature were consistent with that of relative density, indicating that density is the dominating factor to control ϵ_r values in $Li_2Mg_3BO_6$ (B = Ti, Sn, Zr) system. The porosity corrected values (ϵ_{corr}) were generally higher than the measured ones and they behaved a similar tendency, as calculated by the following equation [25]:

$$\epsilon_{meas} = \epsilon_{corr}\left(1 - \frac{3P(\epsilon_{corr} - 1)}{2\epsilon_{corr} + 1}\right) \quad (2)$$

where P is the porosity fraction. On the other hand, the Clausius–Mossotti relationship [26], Eq. (3), can be used to predict the relative permittivity (ϵ_r):

$$\epsilon_r = \frac{(3V_m + 8\pi\alpha_D)}{(3V_m - 4\pi\alpha_D)} \quad (3)$$

here ϵ_r, Vm, and α_D represent the relative permittivity, molar volume, and polarizability, respectively. As given in Table 1, the relative permittivity (ϵ_{theo}) for $Li_2Mg_3BO_6$ (B = Ti, Sn, Zr) ceramics

Table 1
The lattice parameters, packing fraction, and microwave dielectric properties of $Li_2Mg_3BO_6$ (B = Ti, Sn, Zr) ceramics sintered at optimum temperatures.

	$Li_2Mg_3TiO_6$	$Li_2Mg_3SnO_6$	$Li_2Mg_3ZrO_6$
Sintering temperature (°C)	1280	1360	1380
$a = b = c$ (Å)	4.173(5)	4.254(5)	4.293(6)
ϵ_{theo}	6.8	6.1	6.0
ϵ_{corr}	15.4	9.5	14.1
ϵ_{meas}	15.2	8.8	12.6
Packing fraction (%)	53.8	51.1	49.8
$Q \times f$ (GHz)	152000	123000	86000
f_0(GHz)	8.3	10.7	9.3
τ_f(ppm/°C)	−39	−32	−36

were estimated as 6.8, 6.1, and 6.0, respectively. For B = Ti or Zr, the predicted values of permittivity are merely less than half of the measured values of permittivity after correcting the porosity, which suggests that the peculiar crystal chemistry of $Li_2Mg_3BO_6$ enhances the relative permittivity beyond the value expected from the Clausius–Mossotti relationship. Shannon [27] highlighted that large discrepancies between measured and estimated values can be an indication of "rattling" or "compressed" cations with correspondingly high or low polarizabilities, or the presence of dipolar impurities. Indeed, the deviations in this study may be caused by "structural changes", such as local atomic motion or polyhedral distortion. The BO_6 (B = Ti, Sn, Zr) octahedral is composed of O^{2-} ($R = 1.4$ Å) in face centers and B^{4+} in the cubic center. The polyhedron can adjust its configuration to adapt to the small cation by movement of the cation and/or anions resulting in polyhedra distortions [28], which may make larger ion polarizabilities and thus increase the permittivity of $Li_2Mg_3BO_6$ (B = Ti, Sn, Zr) ceramics. The accurate determination of the degree of polyhedral distortion for $Li_2Mg_3BO_6$ (B = Ti, Sn, Zr) ceramics, which is crucial to the investigation of structure-property, deems necessary and will be discussed in the future.

The $Q \times f$ values of $Li_2Mg_3BO_6$ (B = Ti, Sn, Zr) ceramics as a function of sintering temperature are demonstrated in Fig. 4(a). With increasing sintering temperature, $Q \times f$ values of $Li_2Mg_3BO_6$ (B = Ti, Sn, Zr) samples continuously increased to a maximum value and thereafter decreased, exhibiting a similar tendency as the variation in density. Many factors could affect the microwave dielectric loss, which can be categorized as either the intrinsic loss or the extrinsic loss. Intrinsic loss is mainly caused by lattice vibration modes, whereas extrinsic loss is dominated by secondary phases, oxygen vacancies, grain sizes, and densification or porosity [29]. As mentioned above, $Li_2Mg_3TiO_6$ samples possessed high densities of >97% and no secondary phases were detected. These extrinsic impacts on $Q \times f$ could be thus out of consideration. For $Li_2Mg_3BO_6$ (B = Sn, Zr) samples, with increasing sintering temperature, the improvement of $Q \times f$ values can be attributed to increasing of density. It has been reported that the impurities, even in trace amounts, cause an increase in the dielectric loss of ceramics [30]. Further increasing sintered temperature, the changes in stoichiometry derivate from the evaporation of Li would lead to increasing of porosity and the secondary phases (Mg_2SnO_4 and ZrO_2 in $Li_2Mg_3BO_6$ (B = Sn, Zr) ceramics, respectively), which would in turn have a deleterious effect on $Q \times f$ values. The highest $Q \times f$ values of 152,000 GHz (at 8.3 GHz), 123,000 GHz (at 10.7 GHz) and 86,000 GHz (at 9.3 GHz) for $Li_2Mg_3BO_6$ (B = Ti, Sn, Zr) were obtained when each of the materials was synthesized at the corresponding optimal temperature of 1280 °C, 1360 °C and 1380 °C, respectively. To evaluate the variation in the $Q \times f$ values of $Li_2Mg_3BO_6$ (B = Ti, Sn, Zr) ceramics, the packing fraction were calculated using the following formula [31]:

$$\text{packing fraction (\%)} = \frac{\text{volume of packed ions}}{\text{volume of primitive unit cell}} \quad (4)$$

As shown in Table 1, $Li_2Mg_3BO_6$ ceramics with smaller B-site ionic radius atom decreased the unit cell volume, which in turn increased the packing fraction of the specimens. Moreover, a higher packing fraction resulted in a higher $Q \times f$ values as well as a lower densification temperature, a similar phenomenon was reported in the $A_{0.5}Ti_{0.5}NbO_4$ (A = Zn, Co) system [31]. Thus, loss quality was strongly dependent on the atomic packing fraction of specimens in the $Li_2Mg_3BO_6$ (B = Ti, Sn, Zr) system. Furthermore, the curves of τ_f versus firing temperature were given in Fig. 4(b). No remarkable change in τ_f values was found with increasing sintering temperature and they fluctuate around a constant value of approximately −39 ppm/°C for $Li_2Mg_3TiO_6$, −32 ppm/°C for $Li_2Mg_3SnO_6$, and −36 ppm/°C for $Li_2Mg_3ZrO_6$, respectively.

4. Conclusion

A series of $Li_2Mg_3BO_6$ (B = Ti, Sn, Zr) microwave dielectric ceramics were produced by using the conventional solid-state method, and the phase purity, microstructure, and dielectric properties were investigated. The XRD patterns revealed all samples displayed a cubic rock salt structure, and a little of impure phase of Mg_2SnO_4 and ZrO_2 were observed in $Li_2Mg_3SnO_6$ and $Li_2Mg_3ZrO_6$ ceramics, respectively. The samples sintered at 1280 °C (for $Li_2Mg_3TiO_6$), 1360 °C (for $Li_2Mg_3SnO_6$) and 1380 °C (for $Li_2Mg_3ZrO_6$) exhibited excellent microwave dielectric properties: $\epsilon_r = 15.2$, $Q \times f = 152{,}000$ GHz (at 8.3 GHz), $\tau_f = -39$ ppm/°C, $\epsilon_r = 8.8$, $Q \times f = 123{,}000$ GHz (at 10.7 GHz), $\tau_f = -32$ ppm/°C, and $\epsilon_r = 12.6$, $Q \times f = 86{,}000$ GHz (at 9.3 GHz) $\tau_f = -36$ ppm/°C, respectively. The excellent microwave dielectric properties of the $Li_2Mg_3BO_6$ (B = Ti, Sn, Zr) ceramics make them as potential candidates for applications.

Acknowledgments

This work is supported by the National Natural Science Foundation of China (Grant nos. 51272150, 51572162 and 51132003), the Scientific Research Foundation of Shaanxi Normal University (Grant no. X2013YB01, S2012YB05), Specialized Research Fund for the Doctoral Program of Higher Education (No. 20120202110004), and the Fundamental Research Funds for the Central Universities (GK201401003).

References

[1] W. Wersing, Microwave ceramics for resonators and filters, Curr. Opin. Solid State Mater Sci. 1 (1996) 715–731.
[2] J.K. Plourde, D.F. Linn, H.M.J. O'Bryan, J.J. Thompson, $Ba_2Ti_9O_{20}$ as a microwave dielectric resonator, J. Am. Ceram. Soc. 58 (1975) 418–420.
[3] M.T. Sebastian, Dielectric Materials for Wireless Communications, Elseiver Publishers, Oxford, U.K, 2008.
[4] K. Wakino, Miniaturization techniques of microwave components for mobile communications systems—using low loss dielectrics, Ferroelectr. Rev. 22 (2000) 1–49.
[5] G. Subodh, M.T. Sebastian, Microwave dielectric properties of $Sr_2Ce_2Ti_5O_{16}$ ceramic, Mater. Sci. Eng. B 136 (2007) 50–55.
[6] K.P. Surendran, M.T. Sebastian, Low loss dielectrics in $Ba[(Mg_{1/3}Ta_{2/3})_{1-x}Ti_x]O_3$ and $Ba[(Mg_{1-x}Zn_x)_{1/3}Ta_{2/3}]O_3$ systems, J. Mater. Res. 20 (2005) 2019–2026.
[7] G. Subodh, R. Ratheesh, M.V. Jacob, M.T. Sebastian, Microwave dielectric properties and vibrational spectroscopic analysis of $MgTe_2O_5$ ceramics, J. Mater. Res. 23 (2008) 1551–1556.
[8] D. Zhou, H. Wang, L.X. Pang, C.A. Randall, X. Yao, Bi_2O_3-MoO_3 binary system: an alternative ultralow sintering temperature microwave dielectric, J. Am. Ceram. Soc. 92 (2009) 2242–2246.
[9] A. Surjith, R. Ratheesh, Q. High, Ceramics in the $ACe_2(MoO_4)_4$ (A = Ba, Sr and Ca) System for LTCC applications, J. Alloys Compd. 550 (2013) 169–172.
[10] J.J. Bian, D.W. Kim, K.S. Hong, Glass-free LTCC microwave dielectric ceramics, Mater. Res. Bull. 40 (2005) 2120–2129.
[11] S. George, M.T. Sebastian, Synthesis and microwave dielectric properties of novel temperature stable high Q, $Li_2ATi_3O_8$ (A = Mg, Zn) ceramics, J. Am. Ceram. Soc. 93 (2010) 2164–2166.
[12] G.G. Yao, P. Liu, H.W. Zhang, Novel series of low-firing microwave dielectric ceramics: $Ca_5A_4(VO_4)_6$ (A^{2+} = Mg, Zn), J. Am. Ceram. Soc. 96 (2013) 1691–1693.

[13] D. Zhou, C.A. Randall, H. Wang, X. Yao, Microwave dielectric properties of Li_2WO_4 ceramic with ultra-low sintering temperature, J. Am. Ceram. Soc. 94 (2011) 348–350.
[14] C.F. Tseng, P.A. Lin, Microwave dielectric properties of novel glass-free low-firing Li_2CeO_3 ceramics, J. Am. Ceram. Soc. 97 (2014) 1020–1022.
[15] Q. Zeng, W. Li, J.L. Shi, J.K. Guo, M.W. Zuo, W.J. Wu, A new microwave dielectric ceramic for LTCC applications, J. Am. Ceram. Soc. 89 (2006) 1733–1735.
[16] J. Liang, W.Z. Lu, Microwave dielectric properties of Li_2TiO_3 ceramics doped with ZnO-B_2O_3 frit, J. Am. Ceram. Soc. 92 (2009) 952–954.
[17] Z.F. Fu, P. Liu, J.L. Ma, Fabrication nanopowders by high-energy ball-milling and low temperature sintering Li_2TiO_3 microwave dielectrics, Mater. Sci. Eng. B 193 (2015) 32–36.
[18] J.J. Bian, Y.F. Dong, New high *Q* microwave dielectric ceramics with rock salt structures: $(1-x)Li_2TiO_3 + xMgO$ system ($0 \le x \le 0.5$), J. Eurp. Ceram. Soc. 30 (2010) 325–330.
[19] L.X. Pang, D. Zhou, Microwave dielectric properties of low-firing Li2*M*O3 (*M* = Ti, Zr, Sn) ceramics with B_2O_3–CuO addition, J. Am. Ceram. Soc. 93 (2010) 3614–3617.
[20] C.F. Tseng, P.J. Tseng, C.M. Chang, Y.C. Kao, Novel temperature stable Li_2MnO_3 dielectric ceramics with high *Q* for LTCC applications, J. Am. Ceram. Soc. 97 (2014) 1918–1922.
[21] A.N.J. Keulen, J.G. Hoogendam, K. Seshan, J.G. Ommen, J.R.H. van Ross, The role of tin in Li/Sn/MgO catalysts for the oxidative coupling of methane, J. Chem. Soc. Chem. Commun. 21 (1992) 1546–1547.
[22] J. Hauck, Short-range order and superstructures of ternary oxides *AM*O2, *A*2MO3 and *A*5MO6 of monovalent A and multivalent M metals related to the NaCl structure, Acta Crystallogr. Sect. A 36 (1980) 228–237.
[23] Y. Iida, Evaporation of lithium oxide from solid solution of lithium oxide in nickel oxide, J. Am. Ceram. Soc. 43 (1960) 171–172.
[24] C.F. Tseng, Substituting effects of Zn on microstructural characteristics and microwave dielectric properties of $Nd(Co_{1/2}Ti_{1/2})O_3$ ceramics, J. Am.Ceram. Soc. 91 (2008) 4101–4104.
[25] T. Hanai, Theory of the dielectric dispersion due to the interfacial polarization and its application to emulsions, Kolloid Z. 171 (1960) 23–31.
[26] G.D. Mahan, Octupole modifications of the Clausius–Mossotti relation, Solid State Commun. 33 (1980) 797–800.
[27] R. Shannon, Dielectric polarizabilities of Ions in oxides and fluorides, J. Appl. Phys. 73 (1993) 348–366.
[28] J.D. Dunitz, L.E. Orgel, Stereochemistry of ionic solids, Adv. Inorg. Chem. Radiochem. 2 (1960) 1–60.
[29] B.D. Silverman, Microwave absorption in cubic strontium titanate, Phys. Rev. 15 (1962) 1921–1930.
[30] N.M. Alford, S.J. Penn, Sintered alumina with low dielectric loss, J. Appl. Phys. 80 (1996) 5895–5898.
[31] C.F. Tseng, Microwave dielectric properties of low loss microwave dielectric ceramics: $A_{0.5}Ti_{0.5}NbO_4$ (A = Zn, Co), J. Eurp. Ceram. Soc. 34 (2014) 3641–3648.